ELSEVIER

Coordination Chemistry Reviews
198 (2000) 39–59

COORDINATION CHEMISTRY REVIEWS

www.elsevier.com/locate/ccr

Rational molecular design of a catalytic site: engineering of catalytic functions to the myoglobin active site framework

Shin-ichi Ozaki, Toshitaka Matsui, Mark P. Roach, Yoshihito Watanabe *

Institute for Molecular Science, Myodaiji, Okazaki 444-8585, Japan

Received 12 February 1999; accepted 14 December 1999

Contents

* Corresponding author. Tel.: +81-564-55-7430; fax: +81-564-54-2254.
E-mail address: yoshi@ims.ac.jp (Y. Watanabe)

PII: S0010-8545(00)00234-4

Abstract

Proteins that contain the heme prosthetic group are responsible for many different types of catalytic activity. Understanding the mechanisms through which a particular type of catalytic activity is favored over the others remains a significant challenge. Recently, the most common strategy for structure–function studies for a particular enzyme has involved substitution of amino acid residues by site-directed mutagenesis followed by investigations of the effect of the substitution on the catalytic activity of that system. This work describes a significant departure from this common strategy. Instead, we seek to convert a non-enzymatic hemoprotein into one that is capable of catalytic activity. In so doing, we expect to gain an understanding of the general structural requirements for particular enzymatic functions. Comparison of X-ray crystal structures of myoglobin and peroxidases reveals differences in arrangement of amino acid residues in the heme pockets. On the basis of these structural differences and the reaction mechanism of peroxidases, we have rationally designed several myoglobin mutants in order to convert myoglobin into a peroxidase-like enzyme. We have discovered that the location of the distal histidine in the active site provides a critical balance between the formation and subsequent decay of the oxo-ferryl porphyrin radical cation (compound **I**), a catalytic species for one- and two-electron oxidation and oxygen transfer reactions. The mutants prepared in this work have been altered in such a manner that they have permitted compound **I** to be observed in myoglobin for the first time. This allows us to investigate mechanistic details under single turnover conditions by use of double mixing stopped-flow spectroscopy. Furthermore, some of the mutants we have constructed might be useful as good catalysts for asymmetric oxidations. In this short review, we describe our attempts to elucidate structure–function relationships on the activation of the oxygen–oxygen bond of peroxides by hemoproteins.

Keywords: Myoglobin; Peroxidase; Oxo-ferryl porphyrin radical cation; Compound **I**; Sulfoxidation; Epoxidation

1. Introduction

Hemoproteins play versatile roles in biological systems [1]. For example, cytochromes are involved in electron transfer processes in the mitochondrial electron-transport chain [2], and hemoglobin and myoglobin function as a carrier of molecular oxygen (O_2) [3]. Hemoenzymes like cytochrome P450s, peroxidases, catalases, nitric oxide synthases and cytochrome $P450_{nor}$ are responsible for monooxygenations, electron abstraction processes, the dismutation of hydrogen peroxide (H_2O_2), nitric oxide (NO) synthesis, and the reduction of NO, respectively [4–8]. Despite the differences in functions, all of these proteins have iron protoporphyrin IX (heme) as a common prosthetic group. The different functions therefore stem from the differences in the manner that the heme interacts with amino acid residues and small molecules (e.g. substrates) in the active site.

The electron carrier hemoproteins have two strong axial heme iron ligands and usually prevent access for potential substrates [9]. On the other hand, in the case of

globins and hemoenzymes, a residue in the proximal side of heme pocket serves as an axial ligand and the other coordination site on the distal side of the heme is either vacant or occupied by a water molecule, which is easily exchanged for other ligands such as oxygen or hydrogen peroxide [10,11]. For example, the reaction of ferric peroxidases with H_2O_2 results in heterolytic cleavage of the oxygen–oxygen (O–O) bond to produce an oxo-ferryl species ($O{=}Fe^{IV}$) paired with a porphyrin radical cation in horseradish peroxidase (HRP) or a protein radical in cytochrome *c* peroxidase (C*c*P) [12–14]. In the classical peroxidase reaction cycle, this so called compound **I** species, bearing two electron oxidation equivalents with respect to the ferric state, is normally reduced back to the ferric resting state by two sequential one-electron transfer processes from aromatic substrates (peroxidase cycle in Fig. 1), but there are some examples of the two-electron processes associated with ferryl oxygen transfer to substrates such as thioethers (peroxygenase cycle in Fig. 1) [12–15]. In compound **I** formation, the distal histidine is believed to act as a general acid–base catalyst [12,16,17]. X-ray crystal structures of horseradish peroxidase suggest that a positively charged conserved arginine may also help the heterolysis of peroxide, and NMR studies imply that phenylalanines in the distal side are involved in binding of aromatic substrates [18,19]. The X-ray crystal structure of HRP bearing benzhydroxyamine (BHA), a competing substrate of natural phenol and aromatic amine substrates, in the active site is also available in the protein data bank [20]. Therefore, a distinction between globins and hemoenzymes appears to arise from the arrangement of catalytically important amino acid residues in the distal heme pocket.

In order to examine this hypothesis, we have chosen sperm whale myoglobin (Mb) as the framework for our molecular engineering studies. In effect, we are attempting to convert Mb, a carrier of molecular oxygen, into an efficient, peroxide

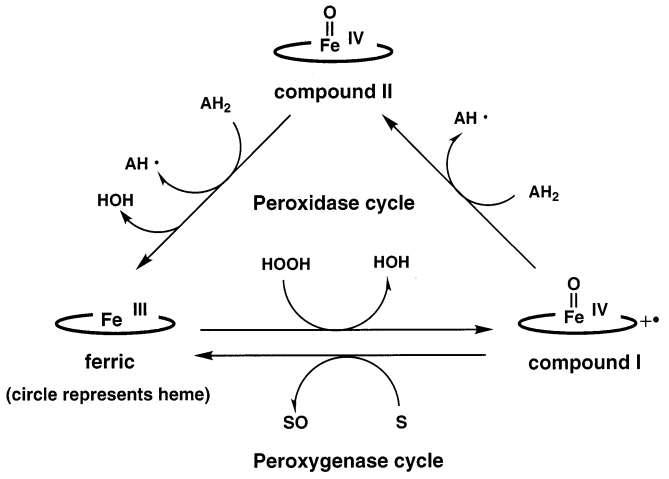

Fig. 1. Peroxidase and peroxygenase cycle. S represents peroxygenase substrates like thioethers and styrenes. AH_2 indicates peroxidase substrates like ABTS and guaiacol.

utilizing hemoenzyme by site-directed mutagenesis. The determination of amino acid sequence of the sperm whale Mb allowed Springer and Sligar to construct the synthetic gene and heterologous expression system in *Escherichia coli* [21]. The X-ray crystal structures of native, wild type, and various myoglobin mutants are now available [11,22–24]. The extensively accumulated biochemical and biophysical data on Mb [25] provide us with a good starting point to probe the structure–function relationships on the activation of peroxides by hemoproteins. In this short review, we describe the rational design, construction, and characterization of Mb mutants accomplished by our research group for the purpose of transforming Mb into an efficient peroxide utilizing hemoenzyme.

2. Rational design of the active site of myoglobin

2.1. Mechanism of compound *I* formation

The crystal structure of cytochrome *c* peroxidase, first obtained in 1980, was the very first peroxidase crystal structure to be solved [17,26,27]. Since then, structures of various peroxidases including horseradish peroxidase (HRP) and chloroperoxidase (CPO) from *Caldariomyces fumago* (*C. fumago*) have been reported (Fig. 2) [17,18,28]. Peroxidases, except for CPO, generally have a proximal histidine as the fifth ligand, and catalytically essential histidine and arginine residues in the distal heme crevice [12,16,29]. On the basis of conservation of certain active site structural aspects, it has been proposed that the distal histidine first functions as a general base to abstract a proton from hydrogen peroxide to allow the binding of the hydroperoxy anion to the heme iron (Fig. 3). Peroxy- or hydroperoxy–heme complexes, postulated as precursors of compound **I**, have been observed for HRP

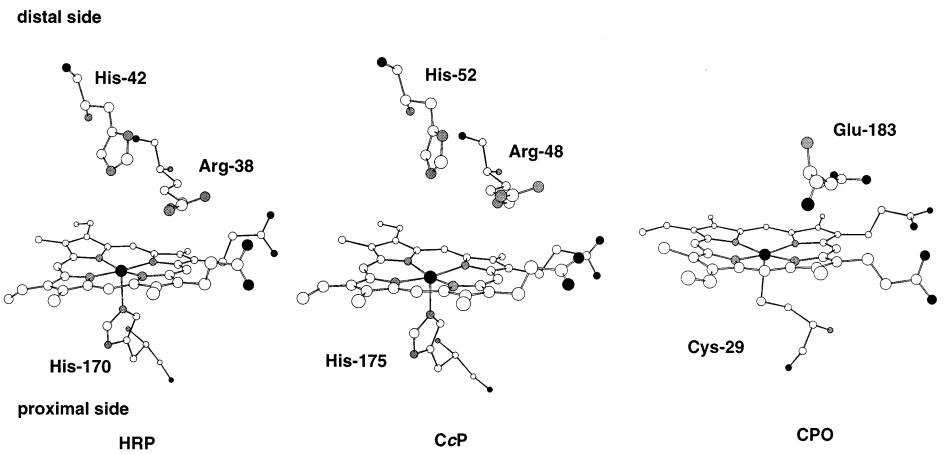

Fig. 2. X-ray crystal structures of horseradish peroxidase (HRP), cytochrome *c* peroxidase (C*c*P), and chloroperoxidase (CPO). Some residues in the heme pocket including proximal ligands are shown.

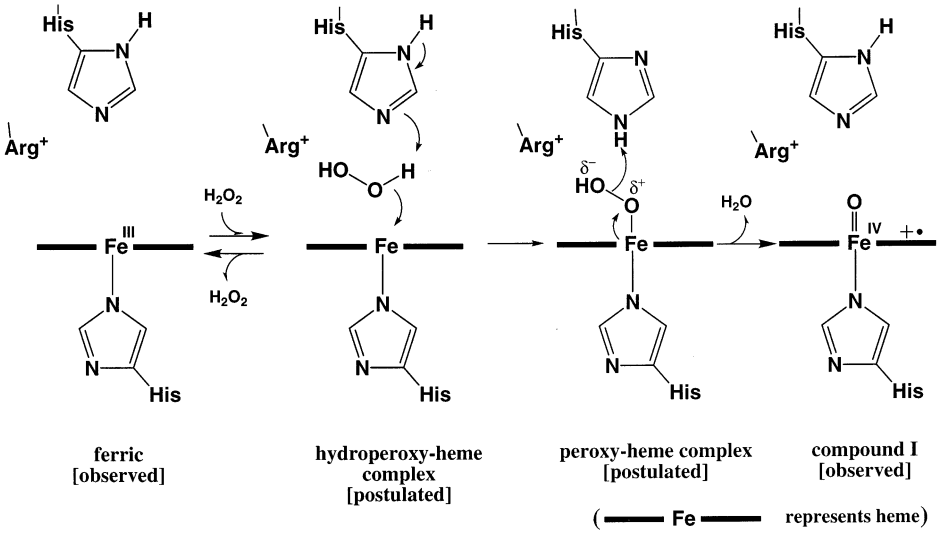

Fig. 3. Proposed mechanism of compound **I** formation. The distal histidine first functions as a general base to deprotonate hydrogen peroxide, and then the protonated histidine as an acid facilitates the O–O bond cleavage.

at low temperature [30–32], and such an intermediate was stabilized by Arg-38 → Leu mutation of HRP [33]. However, more detailed studies are required before a conclusive structural characterization. The protonated histidine then serves as a general acid to facilitate the heterolytic O–O bond cleavage through release of a water molecule. The positively charged distal arginine also induces the polarization of the O–O bond to facilitate the heterolysis. The roles of the distal histidine and arginine are said to exert a 'pull effect'. On the contrary, the anionic proximal histidine stabilizes the transition state of the heterolysis reaction by donating electron density to the heme iron in a so-called 'push effect'. The hydrogen bond between the proximal histidine (His-170) and asparatate (Asp-247) observed in the crystal structure of HRP provides support for the anionic character of the histidine [17,18].

Investigations of the roles of the distal and proximal residues of peroxidases were pursued by replacing residues with other amino acids by site-directed mutagenesis. For example, the mutation of the distal histidine to leucine or valine was found to depress the rate of compound **I** formation from the order of 10^7 to 10^2 or 10 M^{-1} s^{-1} [34–36]. Replacement of the distal arginine with a leucine residue gave the rate constant of 1.5×10^5, which is slower than wild type C*c*P by two orders of magnitude [37]. Studies with HRP have indicated that substitution of the distal arginine by leucine [33,38] or alanine [39] decreases the rate of compound **I** formation by a factor of 10^3. Although mutation of the distal arginine has a smaller impact than deletion of distal histidine, arginine still plays a role in the formation and stabilization of compound **I**. However, the mutation of Asp-247 → Asn in C*c*P

to eliminate the hydrogen bond between the proximal histidine and aspartate did not change the rate of compound **I** formation [40]. Thus, the anionic nature of the proximal histidine ligand does not seem to be crucial for efficient heterolysis to occur. These results suggest that the distal histidine and arginine residues, which provide the pull effect, have a much greater influence on the mechanism of compound **I** formation than the push effect exerted by the anionic proximal histidine ligand.

2.2. Molecular engineering of myoglobin

The mechanism of compound **I** formation for peroxidases postulated on the basis of X-ray crystal structures and site-directed mutagenesis studies implies that it would be possible to rationally design the active site of a catalytically inactive or less active hemoprotein to convert it into a hemoenzyme. Thus, we have attempted to engineer an enzymatic function into myoglobin, a carrier of molecular oxygen.

Comparison of the crystal structures of HRP, C*c*P (Fig. 2) and Mb (Fig. 4) indicates that the distance between N_ε of the distal histidine and ferric heme iron is 4.3 Å in Mb, but the distal histidine in peroxidases lies further away from the heme center (i.e. the distance between N_ε of the distal histidine and iron is 6.0 and 5.6 Å for HRP and C*c*P, respectively) [11,17,18]. Thus, we hypothesize that the distal histidine in Mb is too close to the heme iron to facilitate compound **I** formation and Mb's reactivity with H_2O_2 is consequently lower than that of the peroxidases. The close examination of the crystal structures of the oxy forms of C*c*P and Mb

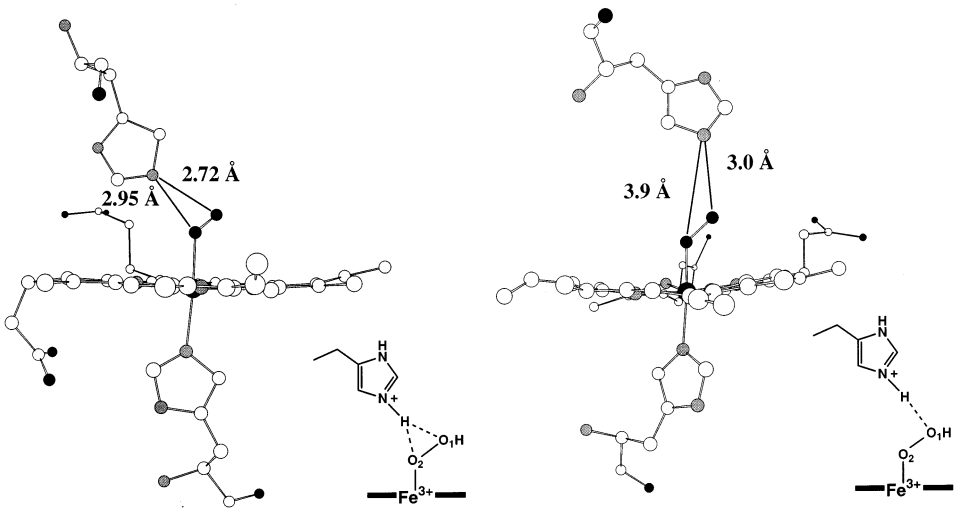

Fig. 4. Comparison of X-ray crystal structures of oxy forms of cytochrome *c* peroxidase (C*c*P) and myoglobin (Mb).

supports our hypothesis (Fig. 4) [41,42]. The distances of the N_ε of the distal histidine and molecular oxygen in oxy-C*c*P are 3.0 Å for the terminal oxygen atom (O1) and 3.9 Å for the oxygen atom bound to the iron (O2), while the values for oxy-Mb are 2.7 and 3.0 Å, respectively. In the reaction of Mb with H_2O_2, the negative charge may not be able to develop on the terminal oxygen atom (O1) to facilitate heterolysis because both oxygen atoms are positioned to accept a proton from N_ε of the distal histidine. In addition, histidine is relatively electron-rich, and is therefore an oxidizable amino acid. Having such a residue in the vicinity of the heme iron might result in rapid electron transfer to the porphyrin oxo-ferryl radical cation (i.e. compound **I** would oxidize the distal histidine rather than substrates through a one-electron transfer from the histidine to the porphyrin) [43–45].

In order to examine our hypothesis, we performed Phe-43 → His/His-64 → Leu (F43H/H64L) and Leu-29 → His/His-64 → Leu (L29H/H64L) double mutations to relocate the distal histidine to a position appropriate for the activation of peroxides. Energy minimization and molecular dynamics calculations predict that the N_ε atom of distal histidine lies at 5.5 and 6.5 Å from the heme iron in the F43H/H64L and L29H/H64L mutant, respectively. Both of these mutants belong to a class called 'distal histidine relocation mutants'. A series of His-64 single mutants has also been made with the objective of prolonging the lifetime of compound **I** in order for it to efficiently react with substrates. Removal of the original oxidizable histidine abolishes a possible pathway for a one-electron reduction of compound **I**. These mutants will be called the 'distal histidine deletion mutants'.

3. Characterization of distal myoglobin mutants

3.1. Functions of the distal histidine in F43H/H64L and L29H/H64L Mb (distal histidine relocation mutants)

The desired mutations were introduced through a polymerase chain reaction (PCR) based technique [46]. The genes of the myoglobin mutants were expressed in *E. coli* and purified from the cell extracts by a previously described procedure [21].

The absorption spectra of ferric F43H/H64L and L29H/H64L Mb exhibit a Soret band at 408 nm, which indicates a typical hexa-coordinated ferric high-spin heme [47,48]. X-ray crystal structures solved at 1.8 Å resolution (Fig. 5) confirm that the sixth ligand is a water molecule stabilized by a hydrogen bond with the distal histidine through another water molecule in the active site [48]. The distance between N_ε of the distal histidine and the ferric heme iron is 5.7 Å in F43H/H64L Mb, which is similar to those in peroxidases (5.5–6.0 Å). In contrast, the distal histidine in L29H/H64L Mb is located farther from heme iron (6.6 Å). Furthermore, hyperfine-shifted ^{1}H-NMR spectra of ferric wild type, L29H/H64L, and F43H/H64L Mb at pD 7.0 reveal that all methyl signals from heme appear in the same region; therefore, introduction of histidines at positions 29 and 43 does not significantly alter the electronic structures of the ferric hemes [48–50].

The reactivity of the myoglobin mutants with hydrogen peroxide was determined from the rate of decay of the ferric state [48]. The rate constant for F43H/H64L Mb is 5.6×10^3 M^{-1} s^{-1}, which is 11-fold greater than the value of the wild type (Table 1). On the contrary, the ferric L29H/H64L mutant shows few changes in the absorption spectrum upon H_2O_2 addition, and we are thus unable to determine the rate constant. It appears that the distal histidine in L29H/H64L Mb lies too far from the heme center to interact with the postulated peroxo iron species, which is a precursor of compound **I**.

In the first step of compound **I** formation, the distal histidine supposedly abstracts a proton from hydrogen peroxide (pK_a 11.6). Since the association of

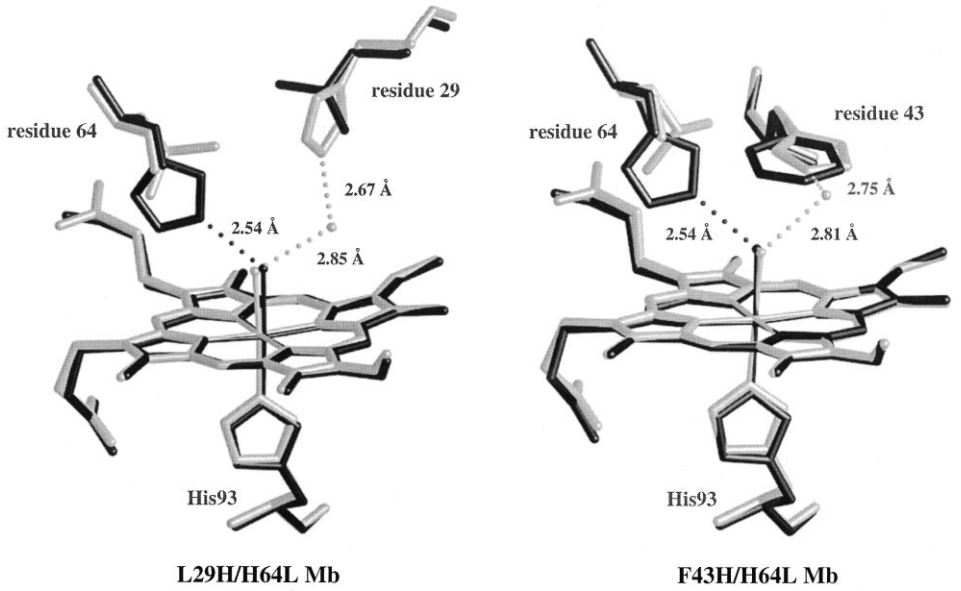

Fig. 5. The X-ray crystal structures of L29H/H64L and F43H/H64L myoglobin mutants (gray: mutants, black: wild type).

Table 1
Reaction of myoglobins with hydrogen peroxide, cyanide, and cumene hydroperoxide (CHP)

	Reaction with H_2O_2[a]	Cyanide association[b]	Heterolysis:homolysis[c]
Wild type Mb	5.1×10^2	0.32	77:23
L29H/H64L Mb	N.D.[d]	0.0081	74:26
F43H/H64L Mb	5.6×10^3	0.88	85:15

[a] The rate constant (M^{-1} s^{-1}) was determined at 20°C.
[b] The association rate constant (M^{-1} s^{-1}) was at 20°C.
[c] The ratio of heterolysis:homolysis was determined from the product ratio (i.e. cumyl alcohol:acetophenone) after 50 min incubation.
[d] The rate constant was too slow to be determined.

cyanide ion (CN^-) also requires the deprotonation of hydrogen cyanide (HCN), the association rate constants of cyanide (k_{CN}) to the ferric state were measured at pH 7.0, at which cyanide is predominately in the protonated form (pK_a 9) (Table 1) [48,51]. The replacement of His-64 with a leucine decreases the rate of cyanide association by 160-fold (k_{CN} for H64L Mb = 0.002 $mM^{-1}\ s^{-1}$) [48]. The introduction of a histidine at the 43 position of H64L Mb accelerates the rate of cyanide binding by 440-fold. Compared to wild type Mb, the rate of cyanide binding is accelerated threefold. The results suggest that the distal histidine of the F43H/H64L mutant functions more effectively as a general base than the distal histidine of the wild type Mb. However, the k_{CN} value of L29H/H64L Mb was 40 times lower than that of the wild type. This is an indication that histidine has been relocated too far from the distal ligand binding site to effectively function as a general base.

In order to examine the ability for the distal histidine to function as a general acid, we next studied the reaction of myoglobins with cumene hydroperoxide (CHP) [48]. The heterolytic O–O bond cleavage of CHP is known to produce compound **I** (or its equivalent) and cumyl alcohol (Eq. (1)), but the homolysis gives compound **II** and cumyloxy radical (Eq. (2)). The subsequent elimination of methyl radical affords acetophenone as a final product (Eq. (3)).

$$Fe^{III}Por + PhC(CH_3)_2OOH \xrightarrow{\text{heterolysis}} Fe^{IV}{=}OPor^{+\bullet} + PhC(CH_3)_2OH \quad (1)$$

$$Fe^{III}Por + PhC(CH_3)_2OOH \xrightarrow{\text{homolysis}} Fe^{IV}{=}OPor + PhC(CH_3)_2O^{\bullet} + H^+ \quad (2)$$

$$PhC(CH_3)_2O^{\bullet} \rightarrow PhCOCH_3 + CH_3^{\bullet} \quad (3)$$

This assay is a useful method to determine the ratio of heterolysis versus homolysis (i.e. cumyl alcohol versus acetophenone) [52]. While the Leu-29 → His/His-64 → Leu mutation does not greatly alter the ratio of heterolysis, approximately 85% of the O–O bond cleavage proceeds heterolytically for the F43H/H64L mutant.

In summary, the distal histidine of F43H/H64L Mb functions as a general acid catalyst, but the wild type His-64 only acts as a general base. Moreover, the His-29 of the L29H/H64L mutant lies too far away for it to efficiently activate the hydrogen peroxide. Consequently, the F43H/H64L mutant reacts the most efficiently with H_2O_2. Our results indicate that the proper positioning of the distal histidine is important for reaction with hydrogen peroxide.

3.2. Peroxidase and peroxygenase activity of the distal histidine relocation myoglobin mutants F43H/H64L and L29H/H64L

Since Phe-43 → His/His-64 → Leu double mutation enhances H_2O_2 activation (cf. Section 3.1), we have investigated oxidations of substrates by this mutant. As depicted in Fig. 1, an oxo-ferryl radical cation can perform two types of oxidations: two sequential one-electron oxidations of substrates such as 2,2′-azinobis(3-ethylbenzothiazoline-6-sulfonic acid (ABTS) and guaiacol, and ferryl oxygen transfer reactions such as sulfoxidations and epoxidations. We call the first type of reaction peroxidase activity and the latter peroxygenase activity (i.e. peroxide dependent monooxygenase activity).

Table 2
Peroxidase activity of myoglobin mutants[a]

	Guaiacol		ABTS	
	V_{max} (turnover min^{-1})	K_m (μM)	V_{max} (turnover min^{-1})	K_m (μM)
Wild type	6.6	570	26	77
L29H/H64L	1.9	76	3.1	11
F43H/H64L	43	99	150	66

[a] The concentration of H_2O_2 is 0.20 mM.

3.2.1. Peroxidase activity

F43H/H64L Mb has approximately six times higher V_{max} values than the wild type both for the guaiacol and ABTS oxidations (Table 2) [48]. In contrast, the L29H/H64L mutant exhibits a V_{max} that is 75% lower than that of the wild type Mb. The changes in the V_{max} values correlate with the reactivities of ferric myoglobins with H_2O_2 (Table 1); therefore, the rate-determining step in the presence of a large excess of substrates appears to be the reaction of the ferric state with hydrogen peroxide. This is consistent with the observation of the ferric species as the steady-state absorption spectrum during the guaiacol oxidation with 4 mM guaiacol [48]. The K_m values for ABTS and guaiacol are in the millimolar range (Table 1). The results imply that the mutations do not appear to improve substrate binding in the active site. Alternatively, the oxidation could occur either at the protein surface as in cytochrome *c* peroxidase (C*c*P) or the heme edge as proposed for horseradish peroxidase (HRP) [53–56].

3.2.2. Peroxygenase activity

Peroxygenation is associated with a peroxide-driven, ferryl oxygen transfer to substrates such as thioethers and styrene. The substrates must have access to the heme pocket. The Phe-43 → His/His-64 → Leu double mutation accelerates the oxidation of thioanisole and styrene by 200- and 300-fold with better enantioselectivity than the wild type (ee (%) > 68%) (Table 3) [57]. The high ^{18}O incorporation from $H_2{}^{18}O_2$ into the sulfoxide and epoxide product clearly indicates ferryl oxygen transfer to the substrates and rules out the involvement of a peroxy protein radical as observed in the epoxidation by C*c*P [56] and wild type Mb (Table 3) [57–60]. Interestingly, L29H/H64L Mb also has better peroxygenase activity than wild type Mb with extremely high enantioselectivity (Table 3) [60]. Since the reactivity of the ferric L29H/H64L Mb with H_2O_2 is much lower than that of the wild type, enhancement of peroxygenase activity for the mutant is not due to the fast formation of an oxo-ferryl radical cation (compound **I**). The results imply that compound **I** of L29H/H64L Mb is capable of catalyzing the oxidation of substrates more efficiently.

Since the oxidation of thioanisole and styrene by the distal histidine relocation mutants has high enantioselectivity, we have explored the scope of asymmetric oxygenation by the use of a various sulfides and styrenes (Table 4) [61]. The

hydroxy group of 2-hydroxymethylsulfide decreases the ee (%) by approximately 25% with respect to ethyl phenyl sulfide, but the *R* enantiomer is still the major sulfoxide product. However, cyclic sulfides give different stereoselectivity from acyclic thioethers for both L29H/H64L and F43H/H64L Mb. The percentage enantiomeric excess in the oxidation of 2,3-dihydrobenzothiophene and 1-thiochroman by L29H/H64L Mb are 67 and 66%, respectively, and the dominant isomers are (*S*)-sulfoxides. On the contrary, *R* is the major enantiomer with 97% enantiomeric excess for thioanisole oxidation by the L29H/H64L mutant. Similar changes in dominant isomers are also observed for F43H/H64L Mb. The L29H/H64L mutant transforms *cis*-β-methyl styrene into the *cis* epoxide with 99% ee (1*R*), but *trans*-β-methyl styrene is oxidized into the *trans* epoxide with 96% ee (1*R*) by F43H/H64L Mb.

On the basis of these changes in stereoselectivity, we postulate the substrate binding mode for the mutants shown in Fig. 6. If we assume the aromatic group is bound in a fixed position, dihydrobenzothiophene and styrene seem to share a common binding orientation. The vinyl group of styrene could orient itself on the same plane of benzene ring to form a flat conformer, whose structure is similar to

Table 3
Enantioselective sulfoxidations and epoxidations by myoglobin mutants[a]

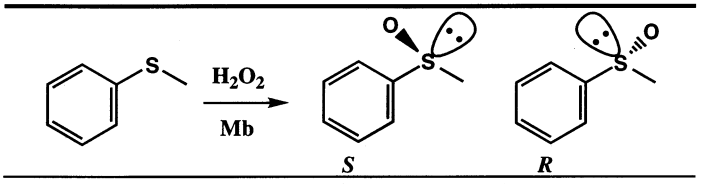

S ***R***

	rate (turnover min^{-1})	% ee	^{18}O incorporation from $H_2{}^{18}O_2$ (%)
wild type	0.25	25 (*R*)	92
L29H/H64L	5.5	97 (*R*)	97
F43H/H64L	47	85 (*R*)	96

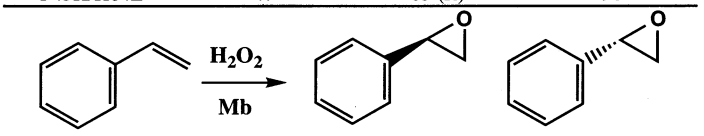

1*R* **1*S***

	rate (turnover min^{-1})	% ee	^{18}O incorporation from $H_2{}^{18}O_2$ (%)
wild type	0.015	9 (*R*)	20
L29H/H64L	0.14	80 (*R*)	94
F43H/H64L	4.5	68 (*R*)	94

[a] The oxidations were performed at 25°C in phosphate buffer, pH 7.0.

Table 4
Asymmetric oxidations by L29H/H64L and F43H/H64L Mb

	wild type Mb		L29H/H64L Mb		F43H/H64L Mb	
	rate[a]	ee(%)	rate[a]	ee(%)	rate[a]	ee(%)
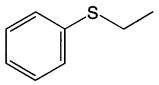	0.46	7.6 (*R*)	6.5	95 (*R*)	26	54 (*R*)
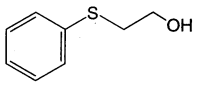	0.65	27 (*R*)	1.6	71 (*R*)	3.2	27 (*R*)
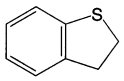	2.2	0.2 (*R*)	24	67 (*S*)	95	17 (*S*)
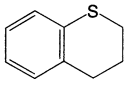	0.8	5.4 (*R*)	3.2	66 (*S*)	50	34 (*S*)
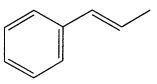	0.076	39 (1*R*, 2*R*)	0.29	83 (1*R*, 2*R*)	16	96 (1*R*, 2*R*)
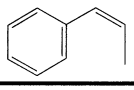	0.0026	3 (1*R*, 2*S*)	0.12	99 (1*R*, 2*S*)	0.15	45 (1*R*, 2*S*)

[a] The unit for rate is turnover min^{-1}.

that of dihydrobenzothiophene. On the contrary, methyl phenyl sulfide approaches the ferryl oxygen with S–CH_3 bond approximately perpendicular to the plane of benzene ring. Energy minimization followed by docking either the substrates or products in the active site of L29H/H64L and F43H/H64L Mb has not immediately provided an obvious rationale for the difference in enantiospecificity. In addition, a relatively large K_m value ($K_m = 9 \pm 2$ mM, $V_{max} = 0.74 \pm 0.1$ turnover min^{-1}) for the L29H/H64L mutant provides a rationale for the failure to simulate the

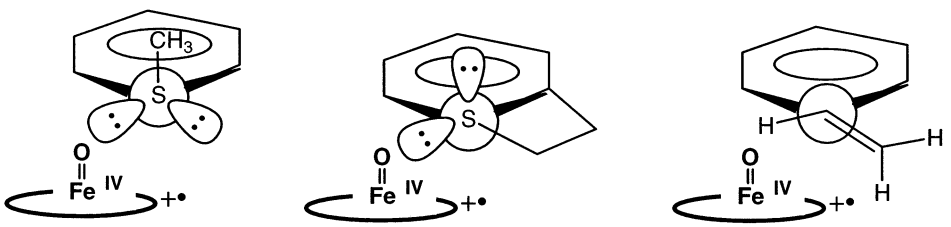

Fig. 6. Postulated substrate binding orientations.

substrate binding mode. Continuous efforts to find substrate analogs (with a smaller K_m value) to mimic a chiral transition state are underway.

3.3. Compound *I* as a catalytic species for the distal histidine relocation myoglobin mutants F43H/H64L and L29H/H64L

The ability of myoglobins to catalyze the sulfoxidation and epoxidation with high ^{18}O incorporation into the products indicates that an oxo-ferryl radical cation (compound **I**) is involved in the catalysis. However, prior to the work described here, compound **I** of wild type Mb had not been successfully observed [62,63]. The reaction of wild type Mb with peroxide gives an absorption spectrum characteristic for an oxo-ferryl species (compound **II**) bearing only one oxidation equivalent with respect to the ferric state, with tryptophan 14 eventually bearing the other oxidation equivalent as a result of leakage of the radical from the porphyrin [64]. More recently, Mason and co-workers reported that tyrosines-103 and -151 are also protein based radical sites and proposed a model in which the unpaired electron density is spread over a number of residues in the population of myoglobin molecules, at least some of which are in equilibrium with each other [65]. This oxidation equivalent might be easily transferred via oxidizable amino acid residues, such as the distal histidine. Compound **II** is also produced directly from the ferric-peroxo complex by homolytic cleavage of the O–O bond as reported in the case of reactions of Mb with peroxides [52,66].

In the L29H/H64L and F43H/H64L mutants we have constructed, the distal histidine is located further away from the iron in order to enhance the rate of formation of compound **I** (Fig. 5). Although L29H/H64L Mb does not efficiently activate hydrogen peroxide, the F43H/H64L mutant reacts with H_2O_2 11 times faster than the wild type (cf. Section 3.1). More importantly, the ratio of heterolysis is improved for F43H/H64L Mb (Table 1). These results motivated us to perform stopped-flow experiments in attempts to detect compound **I** of the mutant. Simple mixing of ferric F43H/H64L Mb and H_2O_2 affords an absorption spectrum of compound **II**. However, the measurement of catalase activity (i.e. $2H_2O_2 \rightarrow O_2 + 2H_2O$, F43H/H64L Mb: 79 ± 2 turnover min^{-1}, the wild type: 1.7 ± 0.2 turnover min^{-1}) suggests that the failure in detecting an oxo-ferryl radical cation could be due to the rapid oxidation of H_2O_2 by compound **I** [6,57]. To circumvent this problem, we used *meta*-chloroperbenzoic acid (*m*CPBA) as an oxidant and were able to observe a compound **I**-type myoglobin species. This represents the first such observation of myoglobin compound **I** [57].

Wild type Mb reacts with *m*CPBA to give compound **II** (Fig. 7(a)); however, a transient intermediate is observed for F43H/H64L Mb under the same conditions (Fig. 7(b)). Upon the mixing of F43H/H64L Mb and *m*CPBA, the absorbance of the Soret band decreases at the rate of $k_{obs1} = 110\ s^{-1}$, and the Soret shifts to 418 nm at the rate of $k_{obs2} = 9.2\ s^{-1}$. The decrease in the Soret band and increase in the absorbance of the 500–700 nm region are characteristic for the conversion of the ferric form to an oxo-ferryl porphyrin radical cation, compound **I** [67]. The species is reduced back to its ferric form upon the addition of thioanisole or styrene, but

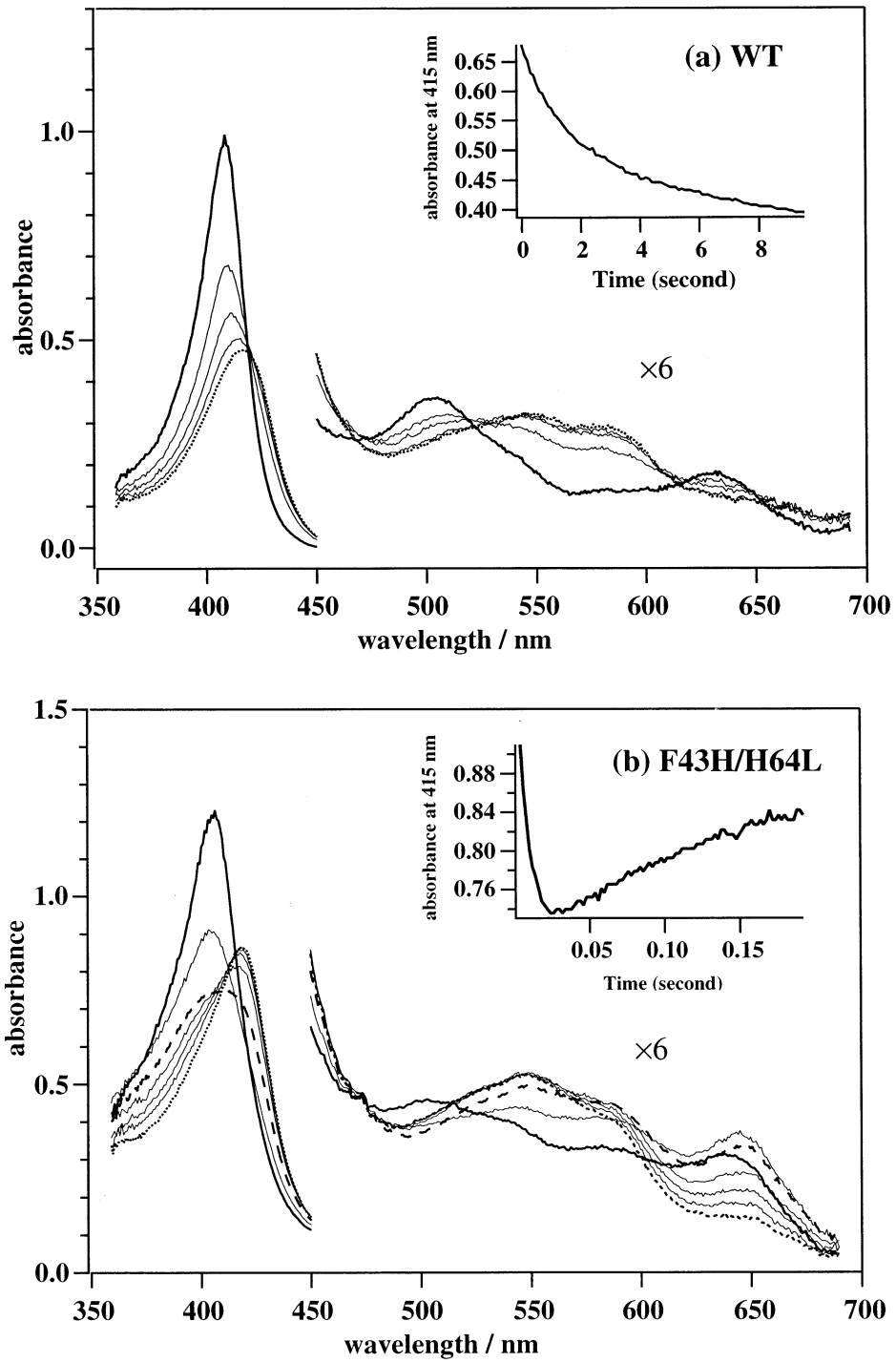
(a) WT
absorbance at 415 nm
Time (second)
×6
absorbance
wavelength / nm
(b) F43H/H64L
absorbance at 415 nm
Time (second)
×6
absorbance
wavelength / nm

Fig. 7.

compound **II** is not accumulated during the reaction. In the absence of substrates, compound **I** decays to compound **II** either by an electron transfer from oxidizable amino acid residues in the heme pocket or by photolysis due to the xenon lamp (a light source for the rapid scan photodiode array) [68]. Compound **I** of L29H/H64L Mb can also be observed upon reaction with *m*CPBA and has been confirmed to have two oxidation equivalents relative to the ferric state [57,61].

Our spectroscopic studies on F43H/H64L and L29H/H64L Mb have clearly identified an oxo-ferryl porphyrin radical cation (compound **I**) as a catalytic species for the peroxygenase activity of these myoglobin mutants. Furthermore, it appears that the proximity of the distal histidine in wild type Mb provides a path for the reduction of the porphyrin cation radical of compound **I** and that its reduction pathway can be eliminated by relocation of the distal histidine.

*3.4. Compound **I** of the distal histidine deletion myoglobin mutants*

The spectroscopic observation of compound **I** of F43H/H64L and L29H/H64L Mb using *meta*-chloroperbenzoic acid (*m*CPBA) as an oxidant raises the possibility that a simple single replacement of the distal histidine might result in greater stabilization of compound **I**. By replacing His-64 with unoxidizable amino acids such as Ala (A), Ser (S), Leu (L), or Asp (D), leakage of oxidation equivalents of compound **I** should be prevented. In peroxide activation, the distal histidine is indispensable as a general acid–base catalyst (cf. Section 2.1); however, as reported in the hemoenzyme model systems [69,70], O–O bond cleavage is exclusively heterolytic due to a good leaving group of peracid (Fig. 8). Therefore, we would be able to observe compound **I** of the distal histidine mutants by use of *m*CPBA.

As expected, we observed compound **I** spectra for the His-64 mutants upon reaction with *m*CPBA (Fig. 9). The rate constants for the formation and reduction of compound **I** are summarized in Table 5 [71]. The rates of compound **I** formation

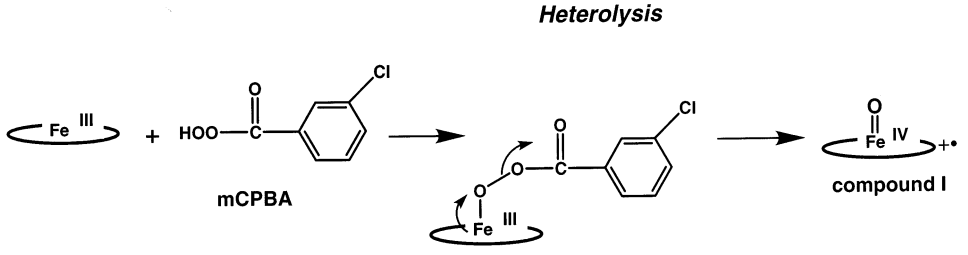

Fig. 8. The reaction of ferric heme with *meta*-chloroperbenzoic acid (*m*CPBA).

Fig. 7. Absorption spectra changes of (a) ferric wild type or (b) F43H/H64L Mb with *m*CPBA in sodium acetate buffer, pH 5.3. Spectra were recorded on a Hi-Tech SF-43 stopped-flow apparatus equipped with MG 6000 diode array spectrometers at 5°C. Insets are changes in absorbance at 415 nm. The black line spectra represent the ferric state. Dashed and dotted line spectra are for compounds **I** and **II**, respectively.

are essentially identical except for that of H64L Mb. Although the reason for the poor reactivity of ferric H64L Mb with *m*CPBA is not clear, it is not due to the steric effect because compound **I** formation of H64L with the less bulky peracetic acid is still slower than H64A Mb (H64L Mb: 7×10^3 M^{-1} s^{-1}, H64A Mb: 3.2×10^5 M^{-1} s^{-1}). The decay rates of compound **I** to **II** (k_{dec}) are essentially the same for the distal histidine deletion mutants (Table 5). Since the k_{dec} value of H64L Mb (0.9 s^{-1}) is approximately ten times less than that for F43H/H64L mutant (9.2 s^{-1}), His-43 of F43H/H64L Mb might provide an electron to reduce compound **I** through the *meso* carbon of the heme as proposed for HRP [72–74].

The rates of compound **I** reduction are essentially identical except for that of H64D Mb (Table 5). Compound **I** of the H64D mutant is reduced back to the ferric state by H_2O_2 approximately three times faster than those of the other His-64 mutants, but thioanisole appears to be a poor substrate for H64D Mb. More interestingly, we can observe the absorption spectrum of compound **I** even upon reaction of H64D with hydrogen peroxide. Although the mechanism of H_2O_2

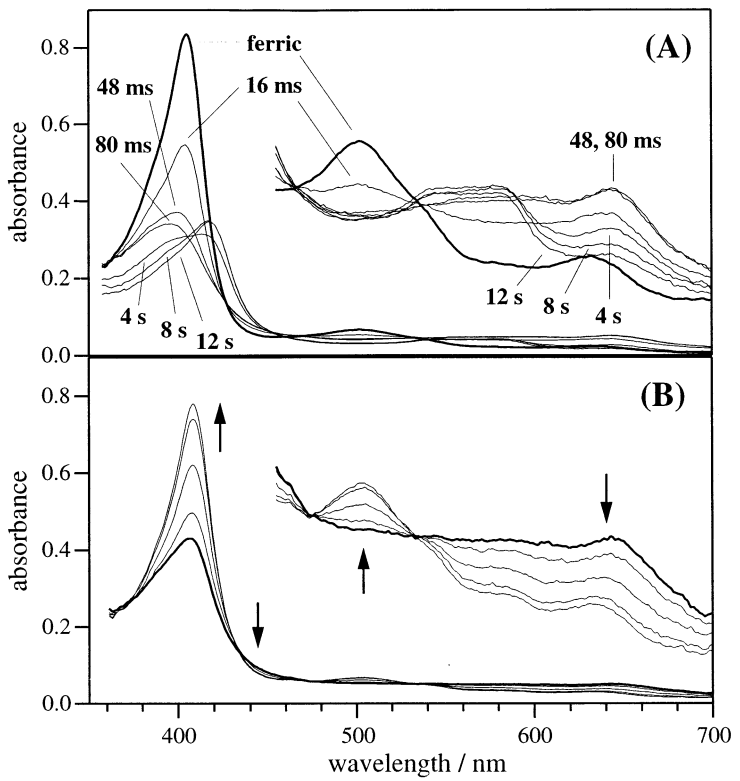

Fig. 9. Absorption spectral changes of H64A Mb upon mixing with *m*CPBA at 5°C in sodium acetate buffer, pH 5.3. (A) Spectra were recorded before addition of *m*CPBA (thick line) and indicated time after mixing in the absence of styrene. (B) Spectra were recorded at 0.10 (thick line) and 0.4–1.3 s after mixing with a 0.3 s time interval in the presence of styrene. The changes in the direction of absorbance are indicated by arrows.

Table 5
Rate constants for the formation (k_1), decay in the absence of substrates (k_{dec}), and reduction (k_2) of myoglobin compound **I**

	k_1 (M^{-1} s^{-1})	k_{dec} (M^{-1} s^{-1})	k_2 (M^{-1} s^{-1})		
			Thioanisole	Styrene	H_2O_2
H64A Mb	4.2×10^5	0.9	1.5×10^6	2.2×10^4	5.9×10^3
H64S Mb	3.0×10^5	0.9	1.5×10^6	2.6×10^4	6.2×10^3
H64D Mb	2.8×10^5	1.2	2.2×10^5	2.1×10^4	1.8×10^4
H64L Mb	1.1×10^4	1.2	N.D.[a]	N.D.[a]	N.D.[a]

[a] The rate constants were not determined because compound **I** of H64L Mb was not generated in the presence of one equivalent of oxidant, and we did not perform the double mixing stopped-flow experiments.

activation without a distal histidine remains unclear, a negatively charged asparatate appears to increase the affinity for H_2O_2 as reflected in the catalase activity (H64D Mb: 160 ± 5 turnover min^{-1} (see also the reduction of compound **I** with H_2O_2 in Table 1). It also should be noted that chloroperoxidase from (CPO) from *C. fumago* has a glutamate on the distal side and a cysteinate proximal ligand (Fig. 2) [28].

4. Combination of distal histidine mutations with proximal heme iron ligand mutations

We have demonstrated that molecular engineering of the distal heme pocket endows Mb with the ability to efficiently activate hydrogen peroxide. However, it is well known at this time that the proximal heme iron ligand also plays a very significant role in peroxide activation for enzymes such as catalases, cytochrome P450s, and chloroperoxidase through exertion of the so-called 'push effect' by which electron density from the anionic proximal ligand facilitates heterolysis of heme iron-bound peroxide [29,75–77]. Bovine liver catalase, perhaps the best characterized of the catalase enzymes, has a proximal tyrosinate ligand and the cytochrome P450s and chloroperoxidase have proximal cysteinate ligands. Mutations of Mb's proximal histidine ligand to tyrosine and cysteine have already been accomplished for human myoglobin [52,78,79] and horse heart myoglobin [80,81] in attempts to duplicate the heme iron coordination structures and reactivities of catalases and cytochrome P450s. A natural extension of the work previously described is to combine the proximal ligand mutations with the distal mutations to produce new structural designs with enhancements in both 'push' and 'pull' effects.

For the proximal tyrosinate series, two mutants were constructed; the triple mutant F43H/H64L/H93Y and the double mutant H64D/H93Y. The purification of both mutants from bacterial cultures was complicated by loss of the heme prosthetic group, an indication that the heme affinity of these mutants is much

lower than that of the wild type and all other mutants discussed here. This problem could be overcome by addition of exogenous hemin to pure or partially pure preparations. The double mutant H64D/H93Y was found to have a stable five-coordinate tyrosinate heme iron coordination structure but, the triple mutant F43H/H64L/H93Y undergoes degradation to a mixture of coordination states that appears to be composed of five-coordinate tyrosinate and a six-coordinate low-spin complex. Somewhat surprisingly, the His-93 → Tyr mutation abolishes the reactivity with H_2O_2. This finding supports the recent hypothesis that the heme iron of Mb is not able to simultaneously bind more than one anionic ligand [82] and also indicates that the role of the tyrosinate ligand in catalase activity still remains unclear.

For the cysteinate series, only one combination mutant, F43H/H64L/H93C, has been produced to date. Again, the mutant incurs a loss of heme during purification and when reconstituted with exogenous hemin, the mutant yields a UV–vis spectrum that resembles that of ferric bis-histidine heme complexes, indicating failure of thiolate ligation. An interesting possibility, which would account for this coordination structure, is that both the newly engineered His43 and the natural His97 are acting as ligands to the heme iron. This new arrangement would require a substantial reorientation of the heme within the heme binding pocket. Again, in this case, the reactivity of the double mutant F43H/H64L with H_2O_2 has been abolished by introduction of the third mutation at the His93 position. Apparently, both histidine ligands are resistant to replacement by exogenous H_2O_2.

More than anything else, these last few examples highlight the possible pitfalls associated with engineering of enzyme systems on an existing heme protein framework and illustrate the importance of extremely subtle interactions which must be considered. In these cases, the length of the proximal ligand tether to the protein backbone and the anionic state of the ligands appear to be of particular significance.

5. Conclusions

We have demonstrated that a close examination of active site structures and reaction mechanism enables us to introduce catalytic ability to myoglobin through a rational design principle. In some cases, peroxygenase activity of mutants is almost comparable to that of peroxidase [83–87]. Efficient chiral catalysts such as F43H/H64L and L29H/H64L Mb might also be useful for asymmetric oxidations of more practical compounds if we can overcome the inactivation that occurs during the reactions. The inactivation appears to be associated with the breach of heme in the presence of an excess of H_2O_2, and we normally observed up to 100 turnovers during the oxidation with the mutants under the steady-state conditions [61]. More importantly, the direct observation of compound **I** of myoglobin mutants gives us an opportunity to investigate details of the peroxygenase mechanism under single turnover conditions as opposed to catalytic conditions [88]. However, the reactivity of ferric F43H/H64L Mb with H_2O_2 is still four orders of

magnitude lower than that of peroxidases. As reported recently [89], random mutagenesis or directed evolution in myoglobin would also be a useful alternative approach to create more efficient enzymes. Our efforts to understand the mechanisms used by natural systems for the activation of peroxides in hemoenzymes is continuing.

References

[1] S.J. Lippard, J.M. Berg, Principles of Bioinorganic Chemistry, University Sciences Books, Mill Valley, CA, 1994.
[2] G.R. Moore, G.W. Pettigrew, Cytochromes C, Springer-Verlag, New York, 1990.
[3] E. Antonini, M. Brunori, Hemoglobin and Myoglobin in Their Reactions with Ligands, North-Holland, Amsterdam, 1971.
[4] P.R. Ortiz de Montellano (Ed.), Cytochrome P450, second ed., Plenum Press, New York, 1995.
[5] J. Everse, K.E. Everse, M.B. Grisham (Eds.), Peroxidases in Chemistry and Biology, vols. I and II, CRC Press, Boca Raton, 1991.
[6] G.R. Schonbaum, B. Chance, in: P.D. Boyer (Ed.), The Enzymes, vol. 13, Academic Press, New York, 1976, pp. 363–408.
[7] O.W. Griffith, D.J. Stuehr, Annu. Rev. Physiol 57 (1995) 707.
[8] S.-Y. Park, H. Shimizu, S. Adachi, A. Nakagawa, I. Tanaka, K. Nakahara, H. Shoun, E. Obayashi, H. Nakamura, T. Iizuka, Y. Shiro, Nat. Struct. Biol. 4 (1997) 827.
[9] G.W. Bushnell, G.V. Louie, G.D. Brayer, J. Mol. Biol. 214 (1990) 585.
[10] R. Liddington, Z. Derewenda, E. Dodson, R. Hubbard, G. Dodson, J. Mol. Biol. 228 (1992) 551.
[11] G.N.J. Phillips, R.M. Arduini, B.A. Springer, S.G. Sligar, Proteins Struct. Funct. Genet. 7 (1990) 358.
[12] H.B. Dunford, in: J. Everse, K.E. Everse, M.B. Grisham (Eds.), Peroxidases in Chemistry and Biology, vol. II, CRC Press, Boca Raton, 1991, pp. 1–24.
[13] P.R. Ortiz de Montellano, Ann. Rev. Pharmacol. Toxicol. 32 (1992) 89.
[14] J.E. Huyett, P.E. Doan, R. Gurbiel, A.L.P. Houseman, M. Sivaraja, D.B. Goodin, B.M. Hoffman, J. Am. Chem. Soc. 117 (1995) 9033.
[15] R.Z. Harris, S.L. Newmyer, P.R. Ortiz de Montellano, J. Biol. Chem. 268 (1993) 1637.
[16] T.L. Poulos, J. Kraut, J. Biol. Chem. 255 (1980) 8199.
[17] T.L. Poulos, S.T. Freer, R.A. Alden, S.L. Edwards, U. Skogland, K. Takio, B. Eriksson, N.-H. Xuong, T. Yonetani, J. Kraut, J. Biol. Chem. 255 (1980) 575.
[18] M. Gajhede, D.J. Schuller, A. Henriksen, A.T. Smithm, T.L. Poulos, Nat. Struct. Biol. 4 (1997) 1032.
[19] G.N. La Mar, G. Hernandez, J.S. de Ropp, Biochemistry 31 (1992) 9158.
[20] A. Henriksen, D. Schuller, K. Meno, K. Welinder, A. Smith, M. Gajhede, Biochemistry 37 (1998) 8054.
[21] B.A. Springer, S.G. Sligar, Proc. Natl. Acad. Sci. USA 84 (1987) 8961.
[22] E.A. Brucker, J.S. Olson, M. Ikeda-Saito, G.N. Phillips, Proteins 30 (1998) 352.
[23] X. Zhao, K. Vyas, B.D. Nguyen, K. Rajarathnam, G.N. La Mar, T. Li, G.N. Phillips, R.F. Eich, J.S. Olson, J. Ling, D.F. Bocian, J. Biol. Chem. 270 (1995) 20763.
[24] J. Kuriyan, S. Wilz, M. Karplus, G.A. Petsko, Mol. Biol. 192 (1986) 133.
[25] B.A. Springer, S.G. Sligar, J.S. Olson, G.N. Phillips Jr., Chem. Rev. 94 (1994) 699.
[26] B.C. Finzel, T.L. Poulos, J. Kraut, J. Biol. Chem. 259 (1984) 13027.
[27] D.B. Goodin, D.E. McRee, Biochemistry 32 (1993) 3313.
[28] M. Sundaramoorthy, J. Terner, T.L. Poulos, Structure 3 (1995) 1367.
[29] J.H. Dawson, Science 240 (1988) 433.
[30] H.K. Baek, H.E. Van Wart, Biochemistry 28 (1989) 5714.
[31] H.K. Baek, H.E. Van Wart, J. Am. Chem. Soc. 114 (1992) 718.

[32] S. Ozaki, Y. Inada, Y. Watanabe, J. Am. Chem. Soc. 120 (1998) 8020.
[33] J.N. Rodorigues-Lopez, A.T. Smith, R.N.F. Thorneley, J. Biol. Chem. 271 (1996) 4023.
[34] S.L. Newmyer, P.R. Ortiz de Montellano, J. Biol. Chem. 270 (1995) 19430.
[35] J.E. Erman, L.B. Vitello, M.A. Miller, J. Kraut, J. Am. Chem. Soc. 114 (1992) 6592.
[36] L.B. Vitello, J.E. Erman, M.A. Miller, J. Wang, J. Kraut, Biochemistry 32 (1993) 9807.
[37] L.B. Vitello, J.E. Erman, M.A. Miller, J.M. Mauro, J. Kraut, Biochemistry 31 (1992) 11524.
[38] J.N. Rodorigues-Lopez, A.T. Smith, R.N.F. Thorneley, J. Biol. Inorg. Chem. 1 (1996) 136.
[39] M. Savenkova, J. Kuo, P. Oritiz de Montellano, Biochemistry 37 (1998) 10828.
[40] J.E. Erman, L.B. Vitello, M.A. Miller, A. Shaw, K.A. Brown, J. Kraut, Biochemistry 32 (1993) 9798.
[41] S.E. Phillips, J. Mol. Biol. 142 (1980) 531.
[42] M.A. Miller, A. Shaw, J. Kraut, Nat. Struct. Biol. 1 (1994) 524.
[43] D. Tew, P.R. Ortiz de Montellano, J. Biol. Chem. 263 (1988) 17880.
[44] A. Wilks, P.R. Ortiz de Montellano, J. Biol. Chem. 267 (1992) 8827.
[45] C.W. Fenwick, A.M. English, J. Am. Chem. Soc. 118 (1996) 12236.
[46] F.M. Ausubel, R. Brent, R.E. Kingston, D.D. Moore, J.G. Seidman, J.A. Smith, K. Struhl, Current Protocols in Molecular Biology, Wiley, New York, 1996.
[47] T. Takano, J. Mol. Biol. 110 (1977) 537.
[48] T. Matsui, S. Ozaki, E. Liong, G.N. Phillips, Y. Watanabe, J. Biol. Chem. 274 (1999) 2838.
[49] K. Rajarathnam, G.N. La Mar, M.L. Chiu, S.G. Sligar, J.P. Singh, K.M. Smith, J. Am. Chem. Soc. 113 (1991) 7886.
[50] M. Ikeda-Saito, H. Hori, L.A. Andersson, R.C. Prince, I.J. Pickering, G.N. George, C.R. Sanders, R.S. Lutz, E.J. McKelvey, R. Mattera, J. Biol. Chem. 267 (1992) 22843.
[51] A. Brancaccio, F. Cutruzzola, C.T. Allocatelli, M. Brunori, S.J. Smerdon, A.J. Wilkinson, Y. Dou, D. Keenan, M. Ikeda-Saito, E. Robert, J. Brantley, J.S. Olson, J. Biol. Chem. 269 (1994) 13843.
[52] S. Adachi, S. Nagano, K. Ishimori, Y. Watanabe, I. Morishima, T. Egawa, T. Kitagawa, R. Makino, Biochemistry 32 (1993) 241.
[53] M.A. Ator, P.R. Ortiz de Montellano, J. Biol. Chem. 262 (1987) 1542.
[54] M.A. Ator, S.K. David, P.R. Ortiz de Montellano, J. Biol. Chem. 262 (1987) 14954.
[55] P.R. Ortiz de Montellano, S.K. David, M.A. Ator, D. Tew, Biochemistry 27 (1988) 5470.
[56] V.P. Miller, G.D. DePillis, J.C. Ferrer, A.G. Mauk, P.R. Ortiz de Montellano, J. Biol. Chem. 267 (1992) 8939.
[57] S. Ozaki, T. Matsui, Y. Watanabe, J. Am. Chem. Soc. 119 (1997) 6666.
[58] P.R. Ortiz de Montellano, C.E. Catalano, J. Biol. Chem. 260 (1985) 9265.
[59] S.I. Rao, A. Wilks, P.R. Ortiz de Montellano, J. Biol. Chem. 268 (1993) 803.
[60] S. Ozaki, T. Matsui, Y. Watanabe, J. Am. Chem. Soc. 118 (1996) 9784.
[61] S. Ozaki, H.-J. Yang, T. Matsu, Y. Goto, Y. Watanabe, Tetrahedron Asymm. 10 (1999) 183.
[62] T. Yonetani, H. Schleyer, J. Biol. Chem. 242 (1967) 1974.
[63] N.K. King, M.E. Winfield, J. Biol. Chem. 238 (1963) 1520.
[64] J.A. DeGray, M.R. Gunther, R. TschirretGuth, P.R. Oritiz de Montellano, R.P. Mason, J. Biol. Chem. 272 (1997) 2359.
[65] M. Gunther, R. Tschirret-Guth, H. Witkowska, Y. Fann, D. Barr, P. Oritiz de Montellano, R. Mason, Biochem. J. 330 (1998) 1292.
[66] A.J. Allentoff, J.L. Bolton, A. Wilks, J.A. Thompson, P.R. Ortiz de Montellano, J. Am. Chem. Soc. 114 (1992) 9744.
[67] D. Dolphin, A. Forman, D.C. Borg, J. Fajer, R.H. Felton, Proc. Natl. Acad. Sci. USA 68 (1971) 614.
[68] J.S. Stillman, M.J. Stillman, H.B. Dunford, Biochem. Biophys. Res. Commun. 63 (1975) 32.
[69] J.T. Groves, R.C. Haushalter, M. Nakamura, T.E. Nemo, B.J. Evans, J. Am. Chem. Soc. 103 (1981) 2884.
[70] J.T. Groves, Y. Watanabe, J. Am. Chem. Soc. 110 (1988) 8443.
[71] T. Matsui, S. Ozaki, Y. Watanabe, J. Biol. Chem. 272 (1997) 32735.
[72] M.A. Ator, P.R. Ortiz de Montellano, J. Biol. Chem. 262 (1987) 1542.
[73] M.A. Ator, S.K. David, P.R. Ortiz de Montellano, J. Biol. Chem. 262 (1987) 14954.

[74] M.A. Ator, S.K. David, P.R. Ortiz de Montellano, J. Biol. Chem. 264 (1989) 9250.
[75] T.L. Poulos, Adv. Inorg. Biochem. 7 (1988) 1.
[76] M. Sono, M.P. Roach, E.D. Coulter, J.H. Dawson, Chem. Rev. 96 (1996) 2841.
[77] Y. Watanabe, in: T. Funabiki (Ed.), Oxygenases and Model Systems, vol. 19, Kluwer, Dordrecht, 1997, pp. 223–282.
[78] S. Adachi, S. Nagano, Y. Watanabe, K. Ishimori, I. Morishima, Biochem. Biophys. Res. Commun. 180 (1991) 138.
[79] T. Matsui, S. Nagano, K. Ishimori, Y. Watanabe, I. Morishima, Biochemistry 35 (1996) 13118.
[80] D.P. Hildebrand, D.L. Burk, R. Maurus, J.C. Ferrer, G.D. Brayer, A.G. Mauk, Biochemistry 34 (1995) 1997.
[81] D.P. Hildebrand, J.C. Ferrer, H.L. Tang, M. Smith, A.G. Mauk, Biochemistry 34 (1995) 11598.
[82] M.P. Roach, S. Franzen, P.S.H. Pang, W.H. Woodruff, S.G. Boxer, J.H. Dawson, in: Y. Ishimura, H. Shimada, M. Suematsu (Eds.), Oxygen Homeostasis and Its Dynamics, vol. 1, Springer-Verlag, Tokyo, 1998, pp. 172–180.
[83] E.J. Allain, L.P. Hager, L. Deng, E.N. Jacobsen, J. Am. Chem. Soc. 115 (1993) 4415.
[84] S.G. Allenmark, M. Andersson, Tetrahedron Asymm. 7 (1996) 1089.
[85] M. Andersson, A. Willetts, S. Allenmark, J. Org. Chem. 62 (1997) 8455.
[86] S. Ozaki, P.R. Ortiz de Montellano, J. Am. Chem. Soc. 116 (1994) 4487.
[87] S. Ozaki, P.R. Ortiz de Montellano, J. Am. Chem. Soc. 117 (1995) 7056.
[88] Y. Goto, Y. Watanabe, S. Fukuzumi, J.P. Jones, J.P. Dinnocenzo, J. Am. Chem. Soc. 120 (1998) 10762.
[89] L. Wan, M. Twitchett, L. Eltis, A. Mauk, M. Smith, Proc. Natl. Acad. Sci. USA 95 (1998) 12825.